ISSN 0023-1584, Kinetics and Catalysis, 2008, Vol. 49, No. 5, pp. 702–707. © Pleiades Publishing, Ltd., 2008.
Original Russian Text © V.V. Molchanov, M.N. Shchuchkin, V.I. Zaikovskii, S.V. Bogdanov, N.A. Zaitseva, 2008, published in Kinetika i Kataliz, 2008, Vol. 49, No. 5, pp. 734–740.

Sorbents and Supports Based on Nanoporous Carbon Xerogels

V. V. Molchanov[a], M. N. Shchuchkin[b], V. I. Zaikovskii[a], S. V. Bogdanov[a], and N. A. Zaitseva[a]

[a] *Boreskov Institute of Catalysis, Siberian Branch, Russian Academy of Sciences, Novosibirsk, 630090 Russia*
e-mail: molchanov@catalysis.nsk.su

[b] *Russian Federal Nuclear Center VNIIEF, Sarov, Nizhni Novgorod oblast, 607188 Russia*

Received June 6, 2007

Abstract—The physicochemical properties of nanoporous carbon materials (TUMaNs) prepared by the carbonization of porous phenol–formaldehyde resin were studied. According to high-resolution electron microscopic data, these materials are nanographites composed of 5- to 10-μm globules, which form chaotically arranged microblocks 3–4 graphene layers in thickness. The materials have a developed system of 1.5- to 3.0-nm micropores and a specific surface area of 450–700 m^2/g. According to X-ray diffraction analysis, the samples consisted of strongly disordered graphite with uniquely large interlayer distances of 0.375–0.390 nm. The sorption properties of TUMaN toward hydrogen and light hydrocarbons were studied. The amount of absorbed hydrogen was higher than analogous values for materials with comparable or even larger specific surface areas. With respect to the sorption of light hydrocarbons, the properties of TUMaN were similar to those of silica and alumina. Nickel supported on TUMaN exhibited an unusually high activity and selectivity in butadiene hydrogenation to butenes. Palladium on TUMaN was highly effective in the hydrofining of ethylene for the removal of acetylene impurities.

DOI: 10.1134/S0023158408050157

INTRODUCTION

Carbon xerogels belong to a new class of technical-grade carbon, which has continuously attracted the attention of specialists in catalysis over the past decade. The increased interest in these carbon materials is due to their unique structure and properties, which are better than those of other carbon materials applicable as sorbents and catalyst supports. Carbon xerogels are formed by the carbonization of phenol–formaldehyde resins, resorcinol–formaldehyde resins, cresol–formaldehyde resins, etc. They have large specific surface areas of 600–700 m^2/g [1, 2]. Activation with oxygen, steam, or carbon dioxide increases the surface area to 1000–1500 m^2/g [1]. By varying the conditions of resin preparation and subsequent carbonization, the ratios between macro-, meso-, and micropores can be varied over wide ranges. These materials are easy to mold, and they can be obtained as thin films, powders, microspheres, etc. The possibility of making irregularly shaped granules is a unique property of carbon supports. The materials exhibit unusually high mechanical strength. The preparation procedure allows one to introduce various metal nanoparticles into a carbon matrix. It is well known from published data that Cr, Mo, W, Fe, Co, Ni, Ru, Pd, Pt, Cu, Ag, Zr, and Ce can be introduced into xerogels [1, 3]. The texture characteristics of these xerogels depend on the nature of the metal. Thus, for example, samples containing small amounts of platinum show meso- and macroporous structures, whereas micropores are more typical of xerogels with palladium and silver additives. The procedure for the preparation of metal–carbon xerogel systems results in the dispersion of metals within a carbon matrix with a well-developed pore structure; that is, this is a method for the synthesis of metal–carbon catalysts. The supporting of metals on carbon xerogels by traditional methods is also well known [4]. A search for the areas of application of these materials is currently in active progress. Data on the use of metal–xerogel systems, which were prepared by either supporting or introducing a metal in the course of xerogel preparation, as catalysts for some reactions are available in the literature. Materials based on carbon xerogels have been used in the manufacture of fuel cell electrodes [5, 6].

To extend the area of application of these materials, in this work we studied the applicability of carbon xerogels as sorbents and supports for metal catalysts. To select samples with optimum characteristics, we studied in detail the physicochemical properties of carbon xerogels containing no metal in the carbon matrix and containing nickel as a constituent. We studied the catalytic properties of nickel-containing carbon xerogels and nickel and palladium catalysts supported on these materials in the reactions of selective hydrocarbon hydrogenation and methane pyrolysis.

EXPERIMENTAL

The samples based on carbon xerogels were synthesized at the Russian Federal Nuclear Center VNIIEF (Sarov) in accordance with a technology developed at this center for the production of nanoporous carbon

Table 1. Compositions for the preparation of carbon xerogels

Component	Component concentrations in the precursors of samples, parts by weight				
	C1	C2	C3	C4	C–Ni
SFZh-302	50	100	200	200	120
Pore-forming agent	100	200	300	300	240
Oxalic acid powder (<200 μm)	100	–	100	100	–
NiO (<50 μm)	–	–	–	–	10

material (TUMaN) by the carbonization of porous phenol–formaldehyde resin [7]. Samples C1–C4 did not contain a metal, whereas nickel was introduced into the carbon matrix of sample C–Ni in the course of sample preparation.

SFZh-302 phenol–formaldehyde resin (OAO Karbolit, Orekhovo-Zuevo) was used to prepare the samples. A system of pores more than 10 nm in diameter was formed by introducing a pore-forming agent, a solution of oxalic acid hexahydrate (30 g) in glycerol (100 g). Table 1 summarizes the compositions of precursors for samples C1–C4 and C–Ni.

After thoroughly mixing the components, the resulting mass was poured in a mold and hardened in a drying oven at 70°C (from 20 to 90 min). The hardened samples were carbonized in a steel container away from air with a uniform increase in the temperature to 900°C at a rate of 6 K/min and then kept at 900°C for no less than 30 min. Upon completion of the carbonization process, the container with the samples was removed from the furnace and cooled away from air. The difference between the preparation of samples C3 and C4 was that the pore-forming agent and oxalic acid were washed from sample C3 after hardening and then carbonization was performed. The Ni/C and Ni/C–Ni supported catalysts were prepared by the incipient wetness impregnation of the supports with aqueous nickel acetate solutions followed by drying in air at room temperature for 24 h and at 110°C for 4 h with subsequent calcination at 350°C for 4 h. Before the determination of catalytic activity, the samples were reduced in a reactor in a flow of hydrogen at 400°C for 1 h.

The Pd/C catalyst was prepared by the incipient wetness impregnation of the support with an aqueous solution of palladium chloride. The sample was dried in air at room temperature for 24 h and at 110°C for 4 h and calcined at 350°C for 4 h. Before the determination of catalytic activity, the sample was reduced in a reactor in a flow of hydrogen at 400°C for 1 h.

The electron micrographs were obtained on a JEM-2010 high-resolution electron microscope with an accelerating voltage of 200 kV and a resolving power of 0.14 nm.

X-ray diffraction analysis was performed on an HZG-4C diffractometer using CuK_α radiation and a graphite monochromator on a diffracted beam. The diffraction patterns were taken by point-by-point scanning over the range of angles $2\theta = 10°–75°$ at a scan step of 0.05°; the accumulation time at a point was 3 s.

The pore structure of the samples was studied by mercury porosimetry with an Autopore 9200 porosimeter (Micrometrics, United States) and using nitrogen adsorption isotherms obtained on an ASAP-2400 instrument (Micrometrics, United States).

The catalytic activity of the Ni/C, C–Ni, and Ni/C–Ni samples in the reaction of butadiene hydrogenation was determined in a flow-circulation system at hydrogen and butadiene flow rates of 7.0 and 1.4 l/h, respectively, over a temperature range of 80–180°C. The catalyst weight was 0.5 g.

The catalytic activity of the C–Ni sample in the reaction of methane decomposition was evaluated in a flow system with a McBain balance from an increase in the sample weight due to carbon formation. The reaction was performed at methane and argon flow rates of 3 and 30 l/h, respectively. The reaction temperature was 350°C, and the catalyst weight was 0.1 g.

The efficiency of the Pd/C sample in the hydrofining of ethylene for the removal of acetylene traces was determined in a flow-type system with a model mixture containing 0.35 vol % acetylene at hydrogen and mixture flow rates of 7.2 and 1.4 l/h, respectively, at 100–120°C. The adsorption of hydrogen was measured on a Sorptomatic-1900 adsorption–desorption apparatus. The isotherms of hydrogen adsorption were measured over the absolute pressure range of 1–1000 Torr at 77 K. Before adsorption measurements, the sample was trained in a vacuum at 300–350°C for 20–24 h.

RESULTS AND DISCUSSION

Physicochemical Properties of the Samples

According to X-ray diffraction analysis data, samples C1–C4 were composed of strongly disordered graphite. This is evident from the occurrence of the two most intense peaks due to a graphite phase (Fig. 1), whereas large diffraction maximum halfwidths (~5° in terms of 2θ) and very large 001 interplanar distances (distances between graphite layers) suggest disorder in the graphite (Table 2).

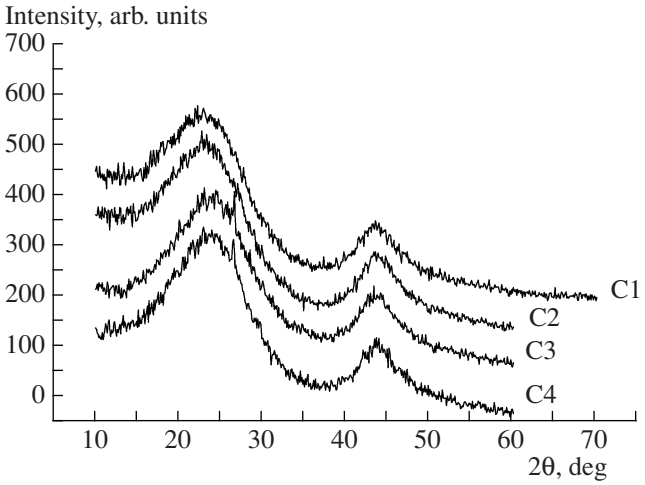

Fig. 1. Diffraction patterns of carbon xerogel samples.

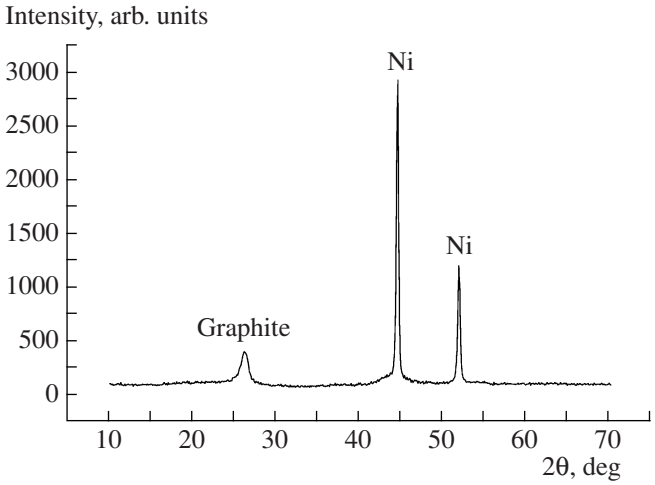

Fig. 2. Diffraction pattern of the sample of a nickel-containing carbon xerogel.

Note that published data on such large distances between graphite layers are unknown.

In the C–Ni sample, the structure of graphite was more ordered; this manifested itself in small diffraction maximum halfwidths (~1°) and interplanar distances close to standard values for graphite (Fig. 2).

In this sample, nickel occurred as a well-crystallized phase; the size of coherent scattering regions was about 70 nm. This size was also supported by electron microscopic data, according to which the shape of nickel particles in the C–Ni sample was near spherical and the particle size varied from 50 to 170 nm (Fig. 3). The major portion of nickel particles exhibited a block structure of 2–4 blocks; as a result of this, the average size of coherent scattering regions was about 70 nm.

According to electron microscopic data, carbon material in samples C1–C4 consisted of globules with a size of 5–10 μm (Fig. 4). These globules exhibited a turbostratic structure formed by chaotically arranged microblocks with sizes of 1–2 nm (Fig. 5a). The space between these blocks can form a system of micropores; this can be seen in the electron micrograph of the surface of a globule (Fig. 5b).

The morphology of carbon in the C–Ni sample containing nickel as a carbon matrix constituent (TUMaN + 9.11% Ni) is of particular interest. The electron micrographs exhibited spherical nickel particles and two types of carbon (Fig. 6). One of them is carbon filaments, and the other is a new morphological carbon species, which was not described previously. It consists of hollow spherical particles with shells 3–4 carbon layers in thickness (Fig. 7). Further study of the properties of the new morphological species is of undoubted scientific and, very likely, practical interest.

Table 2. Interplanar spacing 001 in carbon material samples

Sample	D_{001}
C1	3.87
C2	3.86
C3	3.74
C4	3.74
C–Ni	3.40

According to mercury porosimetry data, the pore structure of the samples consisted of a system of large pores with radii as large as a few tens of micrometers. The volume fraction of pores with sizes larger than 1 μm was more than 95 or 90% in samples C1–C3 or C4, respectively. Because of the small fraction of fine pores (mesopores), the pore size distribution is difficult to determine based on mercury porosimetry data. We can only state that pores with sizes of 30–40 nm occurred in sample C1 (1–2% of the total pore volume), whereas pores with sizes of 150–200, 30–40, and 5–6 nm occurred in sample C2 (1–2% of the total pore volume each). A small fraction of pores with sizes of 150–200 nm occurred in sample C3 in the absence of smaller pores. Finally, a set of pores, which is described by the pore-size distribution diagram shown in Fig. 8, occurred in sample C4. The C–Ni sample exhibited a uniform pore-size distribution over a range of 150 μm–2 nm.

A study of the samples by the method of nitrogen adsorption allowed us to obtain evidence for the microporous structure of carbon material globules, that is, the occurrence of pores with diameters smaller than 2 nm. Table 3 summarizes the results of this study.

Thus, both electron microscopic data and data on nitrogen adsorption suggest that the globules of test carbon materials have a microporous structure with an average pore diameter of 1.5 nm. The high specific surface areas of these materials can be explained by the presence of micropores.

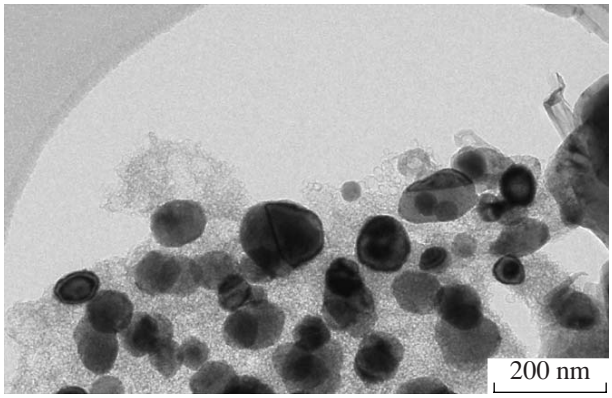

Fig. 3. Electron micrograph of the C–Ni sample.

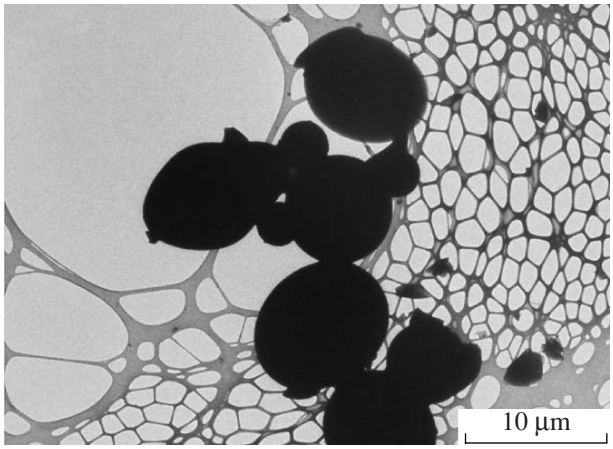

Fig. 4. Electron micrograph of the C2 sample.

Catalytic Properties of Materials Based on Carbon Xerogels in Particular Reactions

We intended to use the C–Ni sample, as well as the Ni/C and Ni/C–Ni supported samples, for the selective hydrogenation of acetylene and butadiene to olefins. These reactions are used to remove the impurities of these compounds from monomers (ethylene and butylene). The hydrogenation of butadiene to butenes was chosen as a model reaction. High selectivity of hydrogenation to olefins was a test for the applicability of catalysts to monomer purification processes.

The C–Ni sample exhibited catalytic properties typical of supported nickel catalysts; that is, it caused deep hydrogenation of butadiene to butane with almost zero selectivity towards butenes. Thus, it is unsuitable for selective hydrogenation reactions; however, it can be used in hydrogenation reactions where high activity is required, for example, the hydrogenation reactions of unsaturated fatty acids (margarine production), the hydrogenation of benzene to cyclohexane, etc. Nickel metal supported onto C–Ni also did not exhibit high selectivity towards butenes in the hydrogenation of butadiene.

Nickel supported on the carbon xerogel that contained no metal as a carbon matrix constituent exhibited an unusually high activity and selectivity in this reaction (Table 4). The reasons for the considerable difference between the catalytic properties of the Ni/C–Ni and Ni/C catalysts remain unknown and invite further investigation.

The supporting of palladium metal on TUMaN allowed us to prepare a catalyst with a low palladium content (0.1% Pd/C), which was highly efficient in the removal of acetylene from ethylene by hydrogenation at 120°C.

To increase the selectivity of catalysts containing iron subgroup metals towards olefins, we developed a procedure that consisted in the carbonization of catalysts prepared by any technique [8]. Although this procedure has been successfully applied previously to the majority of nickel-containing catalysts, it was found to be ineffective in the C–Ni sample for yet unknown reasons. This sample exhibited an unusually low activity, which is uncharacteristic of nickel catalysts, in the pyrolysis of methane. As a result of the reaction, only 1 wt % carbon on the fresh catalyst basis was formed, whereas the increase in weight is usually no lower than

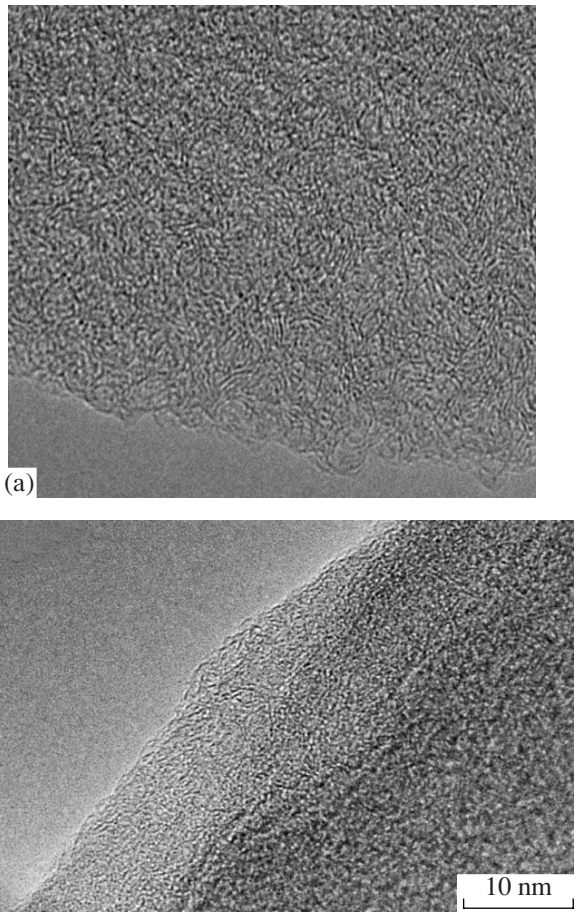

Fig. 5. (a) Turbostratic and (b) microporous structures of the C2 sample according to electron microscopic data.

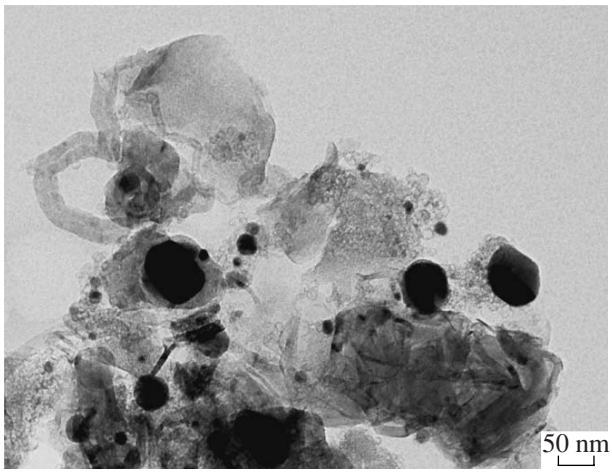

Fig. 6. Electron micrograph of the TUMaN + 9.11% Ni sample.

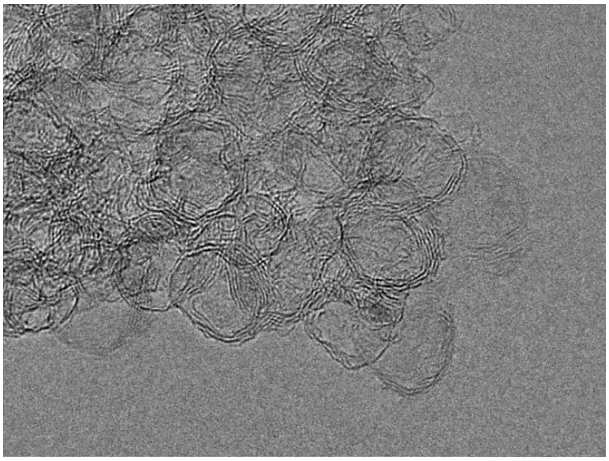

Fig. 7. Electron micrograph of a new morphological species of carbon in the TUMaN + 9.11% Ni sample.

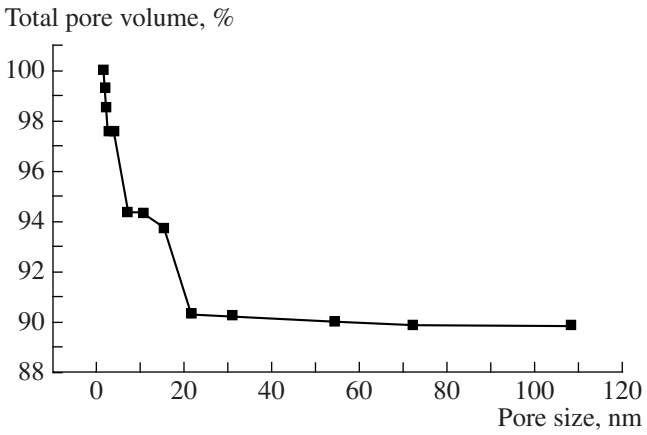

Fig. 8. Pore size distribution of the C4 sample.

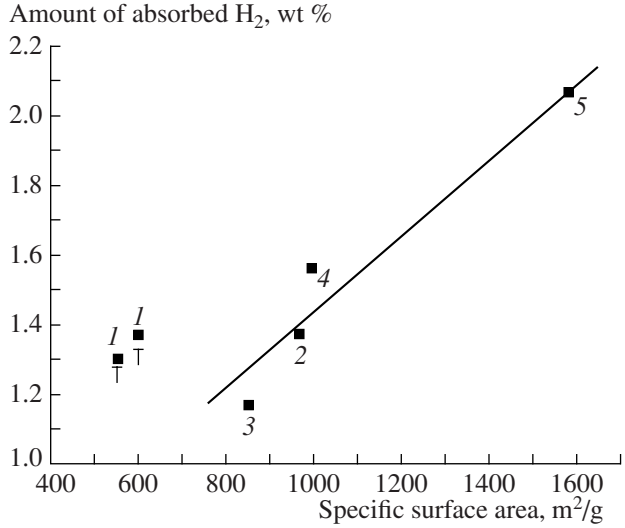

Fig. 9. Hydrogen adsorption capacity of carbon materials specified in Table 5. Point numbers correspond to sample numbers in Table 5. Two points *1* correspond to two different C1 samples.

2000% for nickel catalysts. This low activity cannot be explained by the blocking of nickel particles with carbon because the sample would be fully inactive in a hydrogenation reaction in this case. It is most likely that the reason for the low activity is related to the nature of the carbon in the sample; however, additional studies are required in order to determine this nature. The carbonized sample lost its activity in the hydrogenation reaction. It did not exhibit catalytic properties at reaction temperatures lower than 150°C, and it retained low selectivity toward butenes at higher temperatures with a much lower conversion of butadiene.

The sample containing 5 wt % nickel prepared by the impregnation of a C2 support with a nickel acetate solution was also found to be almost inactive in the reaction of methane decomposition; the increase in weight was 1%. The carbonized sample did not exhibit activity in butadiene hydrogenation over the temperature range 80–200°C. This behavior of supported nickel is very unusual because nickel supported on other carbon supports (Sibunit and filamentous carbon) exhibited high activity in both of the above reactions. Thus, we believe that the most likely reason for the low catalytic activity of nickel is a change in its properties due to its interaction with carbon, which possess other sorption and electronic properties because of its turbostratic structure.

Sorption Properties of Carbon Xerogels

We studied the sorption properties of materials prepared using the TUMaN technology and compared them with the properties of other carbon sorbents.

Table 5 summarizes data on the main texture parameters of the test samples and the values of hydrogen adsorption at 77 K and a pressure of 1 atm.

Table 3. Characteristics of the pore structure of carbon material samples according to nitrogen adsorption data

Sample	Specific surface area, m^2/g	Specific surface area of micropores, m^2/g	Average pore diameter, nm
C1	458	402	1.5
C2	502	461	1.4
C3	570	525	1.4
C4	596	541	1.4
C–Ni	285	211	2.5

Table 4. Catalytic properties of nickel catalysts supported on carbon xerogels in the reaction of butadiene hydrogenation

Catalyst	Reaction temperature*, °C	Selectivity for butenes, mol %	Degree of conversion, %
20% Ni/C	190	98.4	99.4
	205	99.3	99.6
5% Ni/C–Ni	160	72.5	94.0
20% Ni/C–Ni	70	53.2	91.4
20% Ni/Sibunit	70	26.1	99.4

* Optimum reaction temperatures are given for each particular catalyst.

Table 5. Texture parameters and adsorption capacities for hydrogen of carbon sorbents

Entry	Sample	S_{BET}, m^2/g	$V_{micro}(CO_2)$*, cm^3/g	Absorption of H_2, wt %
1	TUMaN	552 ± 8	0.231 ± 0.015	1.30
2	NORIT (commercial sorbent)	968 ± 20	0.256 ± 0.015	1.37
3	PVDC fiber (IPPU, SB RAS)	857 ± 24	0.106 ± 0.010	1.17
4	Fiber (IKhTT, SB RAS)	1000 ± 5	0.245 ± 0.015	1.56
5	SKT 6a (commercial sorbent)	1587 ± 11	0.406 ± 0.020	2.06

* The micropore volume was determined from the adsorption of CO_2.

In Table 5, it can be seen that the TUMaN material stands out sharply against the series of other sorbents: at a much lower specific surface area, it resulted in comparable or even greater absorption of hydrogen, as compared with other carbon materials. This can be seen more clearly in Fig. 9.

With the use of the TUMaN material as a chromatographic sorbent, we found that it is closer in sorption properties to mineral sorbents (alumina and silica) than to carbon materials. For example, this manifested itself in the elution order of light hydrocarbons on passing through a column with this sorbent. The elution orders of light hydrocarbons on three sorbents are given below.

Aktilen-1 acetylene ⟶ ethylene ⟶ ethane ⟶ propylene ⟶ propane,

TUMaN ethane ⟶ propane ⟶ ethylene ⟶ acetylene ~ propylene,

Al_2O_3 ethane ⟶ ethylene ⟶ propane ⟶ propylene ⟶ acetylene.

ACKNOWLEDGMENTS

We are grateful to N.A. Drozdov for the determination of the hydrogen sorption capacity and to V.I. Zheivot for chromatographic studies.

REFERENCES

1. Maldonado-Hodar, F.J., Ferro-Garcia, M.A., Rivera-Utrilla, J., and Moreno-Castilla, C., *Carbon*, 1999, vol. 37, no. 8, p. 1199.
2. Job, N., Pirard, R., Marien, J., and Pirard, J.-P., *Carbon*, 2004, vol. 42, no. 3, p. 619.
3. Moreno-Castilla, C., *"CarboCat 2004," Int. Symp. on Carbon for Catalysis*, Lausanne, 2004, p. 5.
4. Saquing, C.D., Cheng, T.-T., Aindov, M., and Erkey, C., *J. Phys. Chem. B*, 2004, vol. 108, no. 23, p. 7716.
5. US Patent 5601938, 1999.
6. Moreno-Castilla, C. and Maldonado-Hodar, F.J., *Carbon*, 2005, vol. 43, p. 455.
7. RF Patent Appl. 2004134056/15, *Byull. Izobret.*, 2006, no. 13.
8. Molchanov, V.V., Chesnokov, V.V., Buyanov, R.A., et al., *Kinet. Katal.*, 2005, vol. 46, no. 5, p. 701 [*Kinet. Catal.* (Engl. Transl.), vol. 46, no. 5, p. 660].